Vertical Friedel Oscillations in Interface-Induced Surface Charge Modulations of Ultrathin Quantum Islands

W. B. Jian,[1,2] W. B. Su,[1] C. S. Chang,[1] and T. T. Tsong[1,2]

[1]*Institute of Physics, Academia Sinica, Nankang, Taipei, Taiwan, Republic of China*
[2]*Department of Physics, National Taiwan University, Taipei, Taiwan, Republic of China*

(Received 12 June 2002; published 15 May 2003)

Two-dimensional Pb islands of a few atomic layers are grown on the incommensurate Si(111)-Pb surface at low temperatures. Among them, two types of islands having different stacking with the substrate are observed. These islands, respectively, display an alternating image contrast with their thickness. Besides, the contrasts of the islands of different types are complementary to each other layer by layer. These intriguing behaviors do not show significant bias dependence throughout the range from -3 to $+3$ V and can be explained by the vertical charge oscillation with the growth of a new layer. The charge oscillation in the out-of-plane direction originates from electron scattering by the in-plane potential variation at the Pb/Si interface.

DOI: 10.1103/PhysRevLett.90.196603 PACS numbers: 72.10.Fk, 68.37.Ef, 73.21.Fg, 73.61.At

Recently, using electron interference phenomena to image subsurface bubbles [1] and quantized electrons to image buried interface [2,3] and imaging of subsurface dopants in semiconductors [4] have raised questions about charge and density of states oscillations in the vertical direction. For a bound system, when the boundary potential is slightly perturbed, to the first-order approximation [5], it will bring two effects to the confined electrons. One is to cause the energy of the bound states to change in the magnitude of the perturbed potential, while the wave functions are unperturbed but only shift in phase. The buried interface structure can be probed through an individual quantized state near the Fermi level that will display a contrast reversal as imaging across the state [2,3]. This effect is thus of long range and is sensitive to the bias condition. The other effect involves the modification of the wave functions, or the vertical charge density resulted from the integration of all the quantized states modulated by the perturbed potential. Kobayashi [6] considered the 3D tunneling nature of the scanning tunneling microscopy (STM) and proposed a multiscattering model to explain the origin of the subsurface moiré patterns. The charge oscillation will manifest only when the films are thin. Its amplitude starts large and decays as $\sin(2k_F z)/z^2 - \cos(2k_F z)/z$, where z is the film thickness and k_F the Fermi wave vector. Therefore, this effect will dominate in films of a few atomic layers in thickness and will not show a sensitive bias dependence. In order to probe vertical charge oscillations, we have prepared ultrathin metallic films with various thickness on the same substrate. In addition, the interface potential can be further tuned with the help of two reversal stacking sequences of fcc structures in the $\langle 111 \rangle$ direction [7]. Thus, two types of interface-induced vertical charge oscillations, which are bias independent in a wide range, have been found. We believe this is the first experiment to report such a phenomenon.

The clean Si(111)7×7 surface is prepared by flashing the sample to 1500 K in vacuum of base pressure 5×10^{-11} torr. Pb was deposited *in situ* with a mini *e*-beam evaporator. The deposition flux is 0.16 monolayer (ML) per minute. During the deposition, vacuum is maintained at low 10^{-10} torr. The incommensurate (IC) phase is prepared by depositing slightly more than 1 ML of Pb on a clean Si(111) at room temperature with a subsequent flashing to 700 K for a few seconds. After this process, the substrate is turned into a 1×1 bulk-terminated structure with the dangling bonds passivated by Pb atoms. The sample is then cooled to 200 K and subject to further deposition of Pb. STM images are taken right after the deposition with various sample biases.

Figure 1(a) shows a topographic image of Pb islands taken at a sample bias of 2.0 V. In this gray scale presentation, the lowest level (marked 1) is the wetting layer of the IC phase. The next level represents Si islands wetted by Pb, then the two-layer high Pb islands above the IC structure [or three atomic layers (3 AL) in total], and then the 4 AL island. Among the same 3 AL islands, we observed image patterns of several periodicities with the unit cell size ranging from 38.5 Å to less than 25 Å. An atomically resolved image of a 2D Pb island showing 38.5 Å periodicity is displayed in the inset of Fig. 1(a). Because of a mismatch between Si (3.84 Å) and Pb (3.5 Å) lattices, a moiré pattern is generated if one lattice is laid on top of the other. The atomically resolved image can be reproduced by placing 11 Pb atoms above 10 Si atoms, as illustrated in Fig. 1(b). Patterns of other periodicities can also be reproduced in a similar manner with an additional rotation of various angles.

Two types of 3 AL islands with the same period of 38.5 Å exist as seen in Fig. 1(a). The one, marked type I, shows clear image contrast, and the other, type II, barely shows any contrast. To find the cause of this effect, we first examine how their contrast is dependent on the bias. The

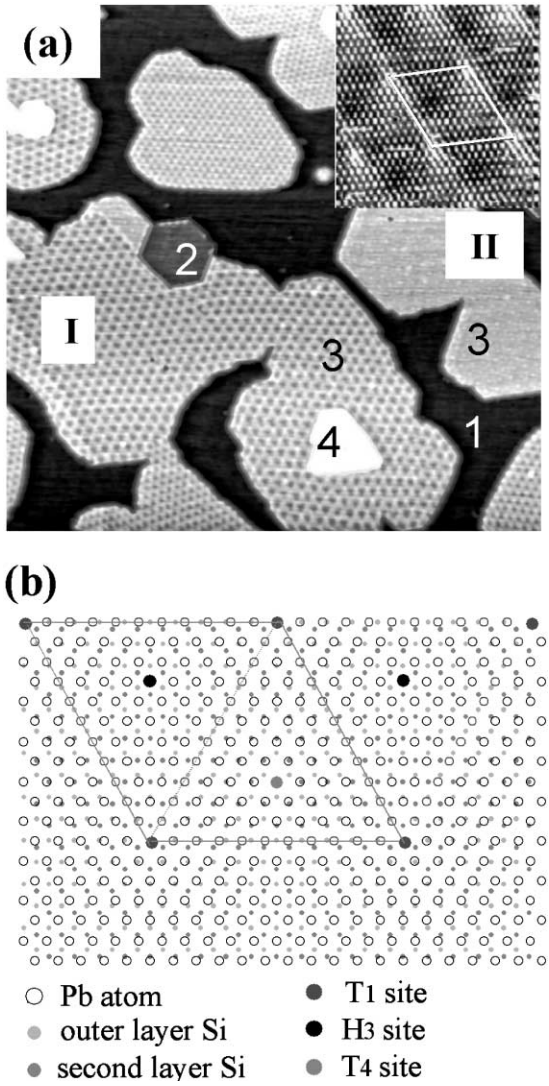

FIG. 1. (a) An STM image (200 nm × 200 nm), taken at a sample bias of +2 V, displays various kinds of surface patterns on the islands of three atomic layers, which are grown on the IC Si(111)-Pb substrate. The periodicities of the patterns range from 22 to 38 Å. Inset: atomically resolved STM image (8 nm × 8 nm), taken at a sample bias of 0.2 V. (b) Sketch for the generation of a moiré pattern with one physical layer of Pb on Si(111). The unit cell is outlined and can be divided into two halves: the T_4 site is in the upward triangular half and the H_3 site is in the downward triangular half.

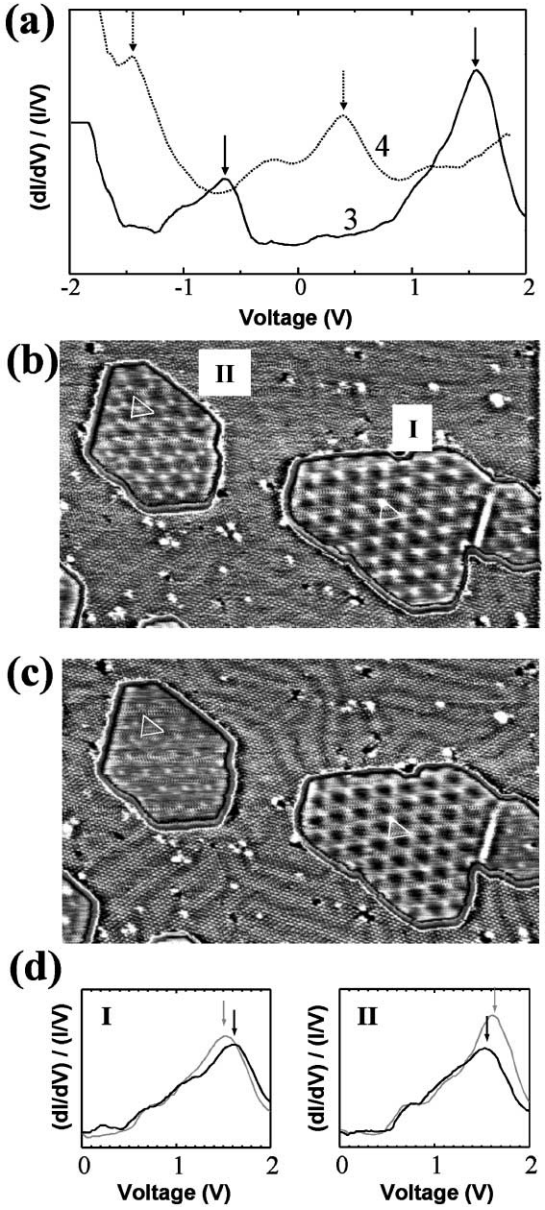

FIG. 2. (a) Averaged dI/dV spectra for the 3 and 4 AL islands. Quantized states are marked with arrows. STM images showing the contrast evolution for the type I and II islands at different biases: (b) 1 V; (c) 2 V. (d) Normalized dI/dV spectra taken at different spots on the 3 AL island. For type I, a quantum state near +1.6 V (black line) appears at the (H_3) site. At the (T_1) site the spectrum (grey line) displays a downward shift of 0.1 V. For type II, a quantum state near +1.6 V (black line) appears at the (T_1) site. At the (H_3) site the spectrum (grey line) displays an upward shift of 0.1 V.

upper triangles in Fig. 2(b), which is taken with the sample bias of 1 V, represent half a unit cell of periodic patterns on both types I and II islands. The highest points located at the corners of the unit cell for type I correspond to the lowest sites for type II. This has been observed, not shown here, on islands combining the two types. We suggest that the highest points for type I are Pb atoms sitting on top of Si atoms (T_1 sites). When the image is taken at 2 V [Fig. 2(c)], we see an enhancement in apparent image contrast differentiating the type I and type II islands. The energy spectrum of the island, as displayed in Fig. 2(a), shows an onset state at 1.6 V. This state originates from the quantized state in the direction normal to the island. The image contrast is much higher for type I than for type II. The change is due to the additional contribution from the quantized electronic state near the Fermi level.

To further investigate the effect of these states on image contrast, we carefully measure the dI/dV spectra at both T_1 and H_3 sites. We obtain the quantum state at sample bias voltage 1.6 V at the H_3 sites. This state shifts to 1.5 V at the T_1 sites for the 3 AL island of type I [Fig. 2(d)]. This implies that the quantum confined waves in the ultrathin film at the T_1 site have a $+\delta$ phase shift relative to quantized waves at the H_3 site. We believe that the physical origin of this shift is due to the relative vertical position between Pb atoms and substrate Si atoms at the interface. With the energy difference, the phase shift δ is estimated to be 15°. This result agrees well with a previous result [3]. The dI/dV spectra for the type II island have also been taken at the corresponding spots as for type I. We discover the state of 1.6 V located at the T_1 sites and an upward shift of 0.1 V for the state near H_3 sites. Thus a phase shift of $-\delta$ at the interface is obtained.

We model the Pb film as a structureless jellium bounded by the vacuum-film and film-substrate interfaces. For electron waves of quantized states scattered by in-plane periodic potential to have a $\pm\delta$ phase shift, the density of state oscillation in the vertical direction to the first-order approximation is proportional to

$$\sin^2(k_z z \pm \delta) - \sin^2(k_z z) \sim \pm\delta \sin(2k_z z), \qquad (1)$$

where k_z is the wave vector and z is a vertical distance from the interface. The vertical charge oscillation is then the summation of all quantized states, which is proportional to $\pm\delta[1 - \cos(2k_F z)]/2z$. Vertical charge oscillations have to be emphasized since we do not observe any image contrast reversal throughout the bias voltage range from -3 to $+3$ V. This phenomenon observed by us in ultrathin films is completely different from imaging the interface by quantized electrons in thicker films [3]. There only a single quantized state nearest to the sample bias voltage dominates. For type II a negative phase shift produces a complementary image contrast as compared to a positive phase shift for type I. The brightest sites in a unit cell for the type I island, therefore, correspond to the darkest sites for type II.

The apparent height difference between the top and the valley can be as large as 0.7 Å in the superstructures imaged at the top of the Pb islands in Fig. 1(a). Focusing on type I islands, when we continue to deposit Pb, the islands will grow layer by layer in the z direction at 200 K. As one more layer grows on top of the island, its contrast turns dim and its morphology reverses as shown in Fig. 3(a). The contrast becomes strong again on the 5 AL island and becomes weak again on the 6 AL. The image morphology on the 5 AL is the same as that on the 3 AL while the apparent corrugation reduces to 0.4 Å. This is similar to the bilayer image contrast oscillation seen with the Pb/Si(111) system [2,8]. The Fermi wavelength along the $\langle 111 \rangle$ direction for the Pb crystal

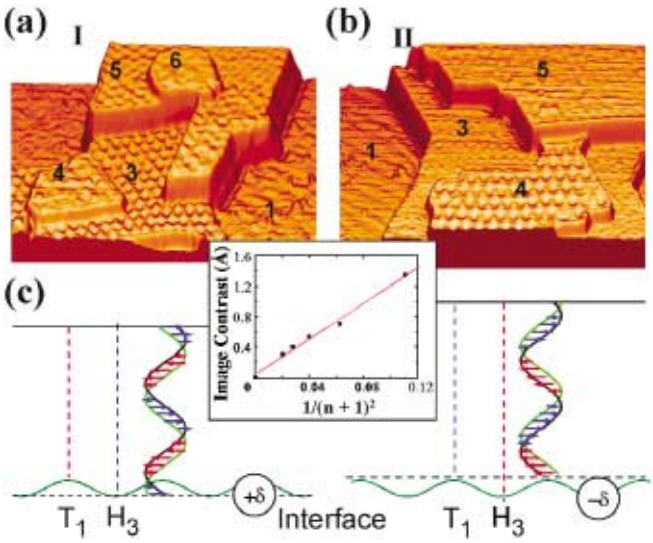

FIG. 3 (color). Properties of the type I island are shown in (a) and (b). (a) STM image (120 nm × 60 nm), taken at a sample bias voltage of +2 V, showing patterns on 3–6 layer-high islands of type I (see text). (b) STM image (120 nm × 60 nm), taken at a sample bias voltage of +2 V, showing patterns on 3–5 layer-high islands of type II (see text). (c) A schematic drawing illustrates the phase shift and charge oscillations at different sites where the shifted quantized state was measured for both type I and II islands. Inset: the amplitude of image contrast is linearly dependent on $1/(n + 1)^2$, where n is the number of atomic layers of Pb islands and the effective width for the bound electrons needs to add one extra layer.

is 3.94 Å [9] and the interlayer spacing d_0 is 2.85 Å. The image morphology reverses with one more layer because there is an additional phase of $2k_F d_0 \sim 3\pi$. For type II islands, reverse pattern oscillations are observed in the z direction as well [Fig. 3(b)]. There, clear image patterns emerge on an even number of AL's while fuzzy patterns emerge on odd number layers, just complementary to what is observed for type I. The apparent height differences are 1.35, 0.54, and 0.3 Å on the 2, 4, and 6 AL, respectively. The apparent contrast shows an oscillating and decaying intensity as the film becomes thicker. The decaying power for both types of islands is close to 2, as shown in the inset of Fig. 3. This is deviated from our simplified model and Kobayashi's derivation where the $1/z$ dependence is the dominant term for thin films. However, if the screening effect is taken into account, the decay of the image contrast should be faster than $1/z$. Furthermore, the screening strength in the thin film may be thickness dependent; as the film grows thicker, it will thus modify the phase shift δ and make the decay toward $1/z^2$ as our model implies. The interface potential, inducing opposite phase shifts of electron waves, is illustrated in Fig. 3(c). A small height difference between types I and II inferred in the figure has been observed in our experiment, but is not shown in this paper.

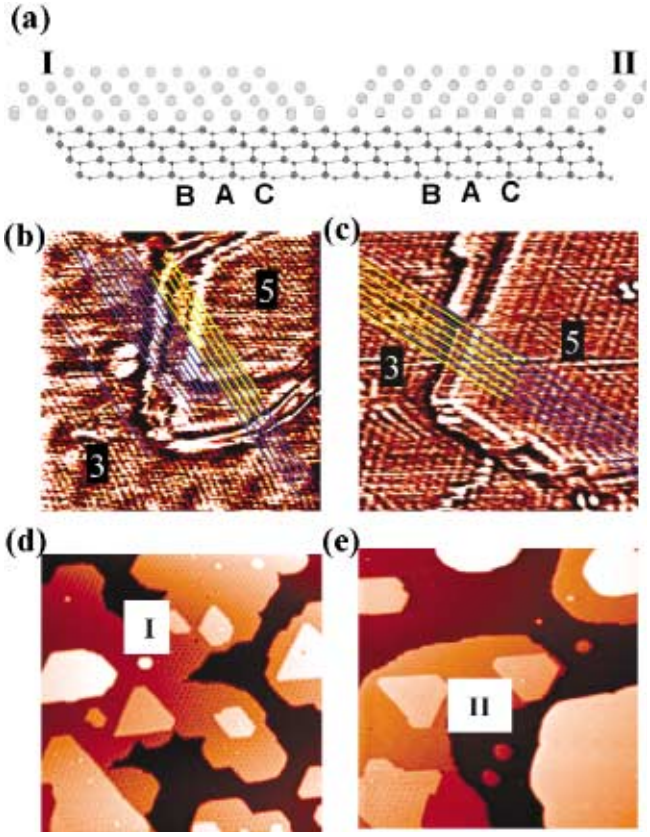

FIG. 4 (color). (a) The side view of geometric models represents the most possible configuration of type I and II islands with emphasis of different stacking. (b) Atomic rows mismatch between the 3 and the 5 AL in the type I island. (c) Atomic rows mismatch on the 3 and the 5 AL in the type II island. (d) Islands of upward triangular shape grown on the 3 AL island of type I. (e) Islands of downward triangular shape grown on the 3 AL island of type II.

The difference between types I and II is due to a different stacking sequence at the Pb/Si interface. Once the topmost Si atoms are wetted by Pb adatoms, the subsequent stacking of Pb atoms in the growing islands can take two different routes. Near the T_1 sites one will follow the Si stacking of aA, bB, cC', A', B', C', . . .; those letters with a prime represent the Pb layers. The other has the sequence of aA, bB, cC', B', C', A', ... The fact that the substrate Si atoms were able to interact with the second layer Pb has caused the electronic states to be different at the interface for the two types of islands [referring to Fig. 2(b)]. To confirm this view, we first take STM images of crossing two atomic layers for both types of islands to examine their stacking sequence. For the fcc crystal, lines of atomic rows will not match each other after crossing two atomic layers, and this is indeed what we saw [Figs. 4(b) and 4(c)]. Secondly, the 4 AL islands of type I prefer to have an upward triangular shape while those of type II tend to have a downward triangular shape [Figs. 4(d) and 4(e)]. It is well known that the formation of triangular islands on a (111) substrate can result in an anisotropic surface diffusion on different facets [10]. The discrepancy in stacking sequence will cause the islands to form into just opposite triangular shapes.

Type I and II islands have the same fcc crystal structures but an opposite stacking sequence thus having different structures at the interface. The opposite stacking can possibly introduce a phase shift to the electrons scattered at the interface and bring forth the complementary vertical charge oscillations between type I and II islands. Concordantly, the charge oscillations all decay monotonically with film thickness and vanish rapidly. Thus for thick films, a similar image contrast cannot be observed. This is the first time vertical charge oscillations have been observed experimentally although, in contrast, the lateral charge oscillations forming standing waves in a two-dimensional electron gas were shown earlier [11]. And not only is the image morphology reversed but also the contrast intensity for both type I and II islands. Until now we consider only the potential induced charge oscillations in the z direction and their magnitude is empirically proportional to $[a \pm \sin(2k_F z)]/z^2$ with the condition of $a < 1$. We believe that the cause of the parameter a is due to a charge neutralization from in-plane electrons. Our interpretation needs to be confirmed by theoretical calculations. We also discovered the observed local charge variation, differing from density of states variation, can affect further growth on the surfaces of ultrathin films.

We acknowledge helpful discussions with C. M. Wei and M. Y. Chou. This study was supported by the National Science Council and Academia Sinica of Taiwan.

[1] M. Schmid, W. Hebenstreit, P. Varga, and S. Crampin, Phys. Rev. Lett. **76**, 2298 (1996).
[2] I. B. Altfeder, D. M. Chen, and K. A. Matveev, Phys. Rev. Lett. **80**, 4895 (1998).
[3] I. B. Altfeder, V. Narayanamurti, and D. M. Chen, Phys. Rev. Lett. **88**, 206801 (2002).
[4] M. C. M. M. van der Wielen, A. J. A. van Roij, and H. van Kempen, Phys. Rev. Lett. **76**, 1075 (1996).
[5] G. Baym, *Lectures on Quantum Mechanics* (Benjamin, New York, 1973).
[6] K. Kobayashi, Phys. Rev. B **53**, 11091 (1996).
[7] P. B. Howes, K. A. Edwards, J. E. Macdonald, T. Hibma, T. Bootsma, M. A. James, and C. L. Nicklin, Surf. Rev. Lett. **5**, 163 (1998).
[8] W. B. Su, S. H. Chang, W. B. Jian, C. S. Chang, L. J. Chen, and Tien T. Tsong, Phys. Rev. Lett. **86**, 5116 (2001).
[9] M. Jalochowski, H. Knoppe, G. Lilienkamp, and E. Bauer, Phys. Rev. B **46**, 4693 (1992).
[10] T. Y. Fu, Y. R. Tzeng, and Tien T. Tsong, Phys. Rev. B **54**, 5932 (1996).
[11] M. F. Crommie, C. P. Lutz, and D. M. Eigler, Nature (London) **363**, 524 (1993).